

Image reconstruction algorithms for microtomography

Andrei V. Bronnikov

Bronnikov Algorithms, The Netherlands

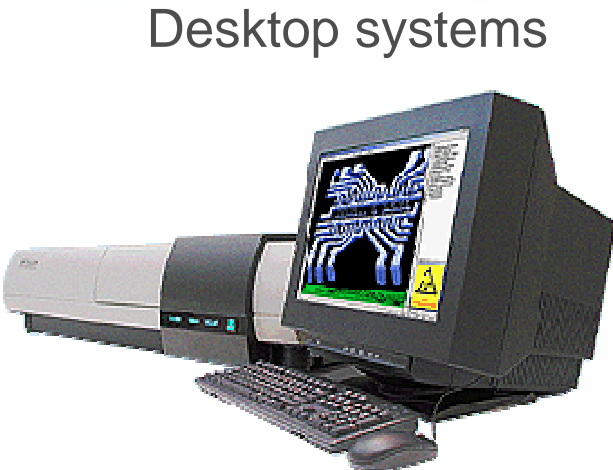
Contents

- Introduction
- Fundamentals of the algorithms
- State-of-the-art in 3D image reconstruction
- Phase-contrast image reconstruction
- Summary

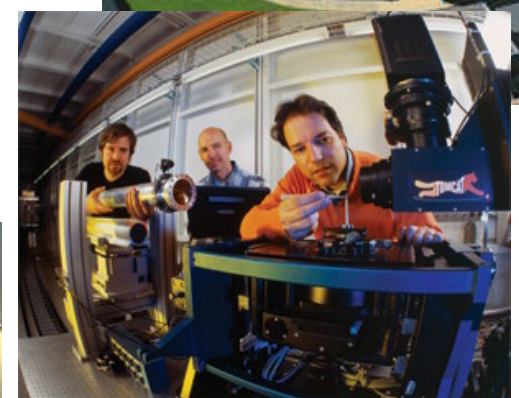
Microtomography systems



NDT systems



Desktop systems



Dental CBCT



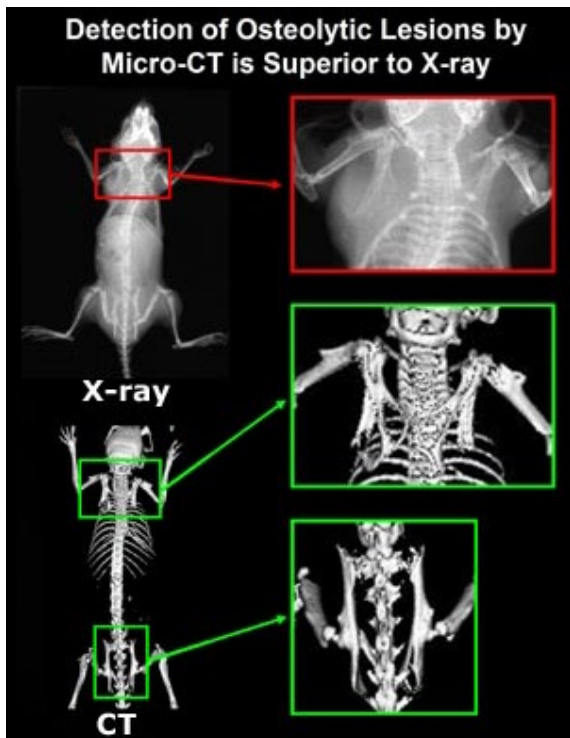
Small animal CT



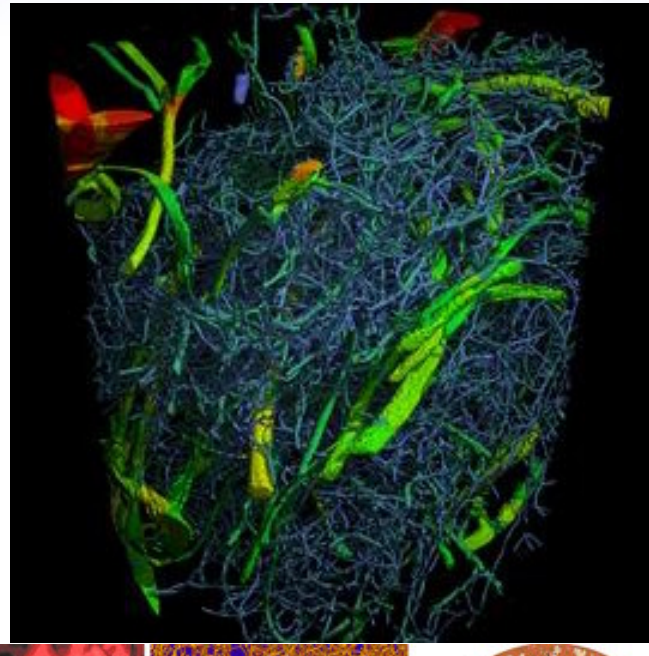
Synchrotron setup

Micro CT images

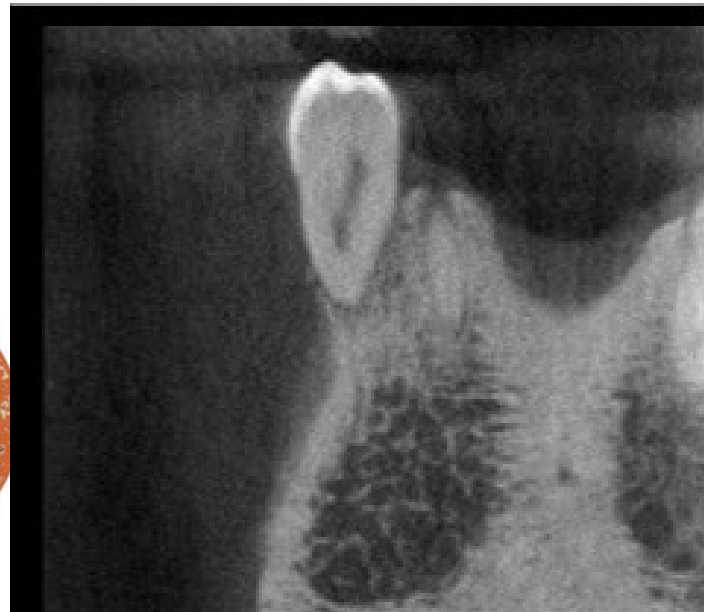
72



Sterling *et al*



Stampanoni *et al*



Dental CBCT

Problems

- Object preparation, fixation, irradiation, etc
- Polychromatic source, miscalibrations, etc
- Small object size: insufficient absorption contrast
- Limited field-of-view, limited data, incomplete geometry
- Large amount of digital data

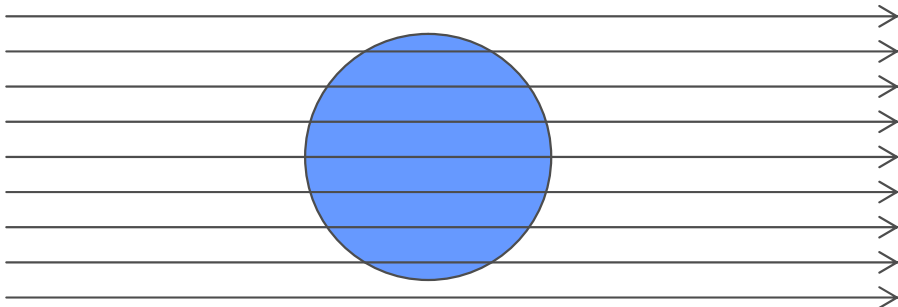
Solutions

- Region-of-interest reconstruction
- Fully 3D cone-beam scanning and reconstruction
- The use of phase contrast
- Software/hardware acceleration

Geometry

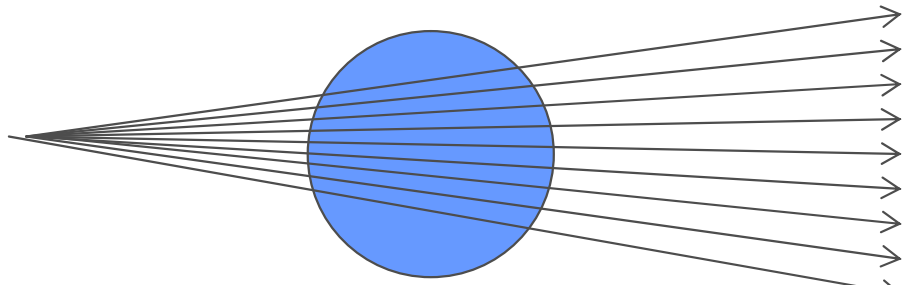
Synchrotron

Parallel beam
The source is far away from the object



Microfocus tube,
microscopy

Cone beam
The source is close to the object:
- Increased flux
- Magnification
- Fully 3D



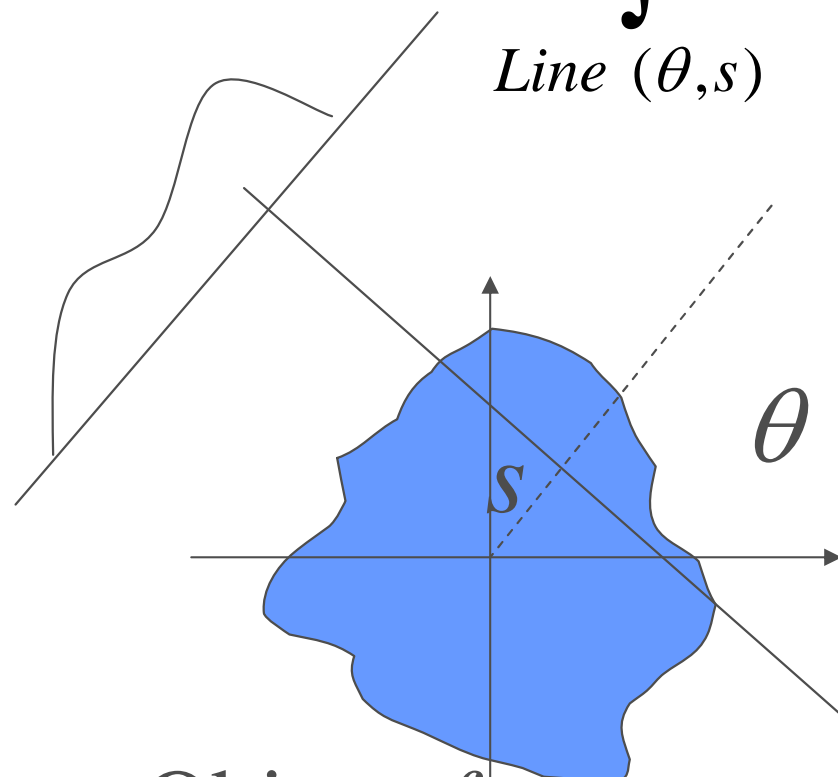
Inverse problem

Projection

data:

$$g_{\theta,s} = \int f \, dl$$

Line (θ,s)



Object: f

Radon transform

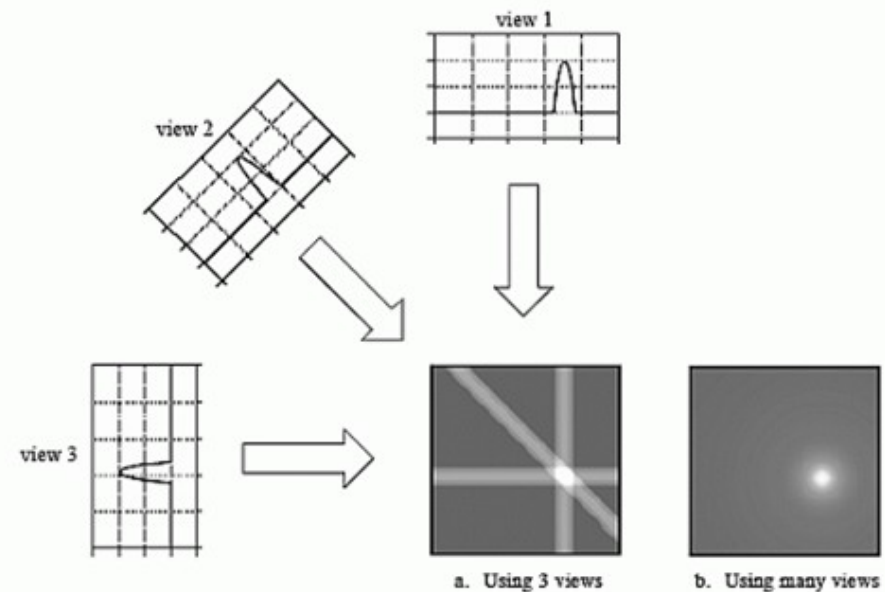
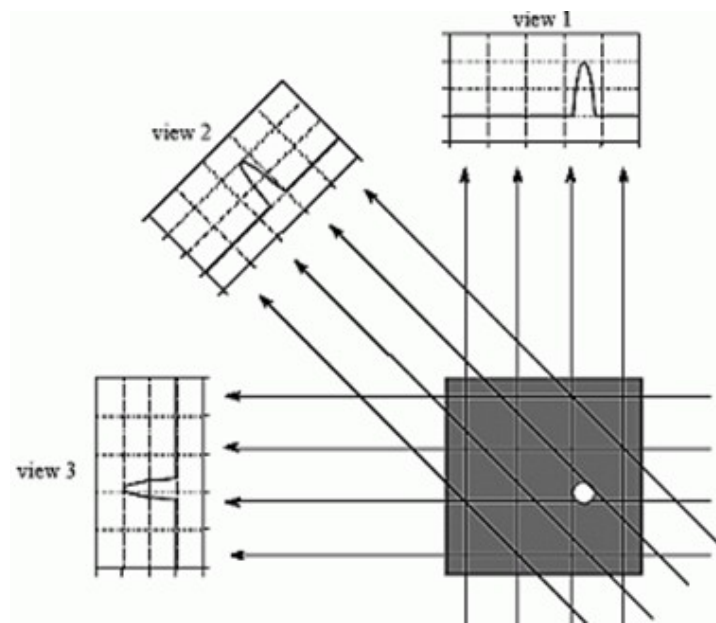
$$Af = g$$

To find f from g ?

Backprojection

Integration of the projection data
over the whole range of θ

$$A^* g = \frac{1}{\pi} \int_0^\pi g \, d\theta$$



Algorithms: classification

- Fourier algorithm
- Filtered backprojection (FBP)
- Backprojection and filtering (BPF)
- Iterative

Radon transform

$$Af = g$$

$$\begin{aligned}f &= (A^* A)^{-1} A^* g \\&= A^* (A A^*)^{-1} g \\&= F_n^{-1} F_{n-1} g\end{aligned}$$

Imaging
equation

BPF

FBP

Fourier

Parallel-beam geometry (Synchrotron)

Fourier slice theorem

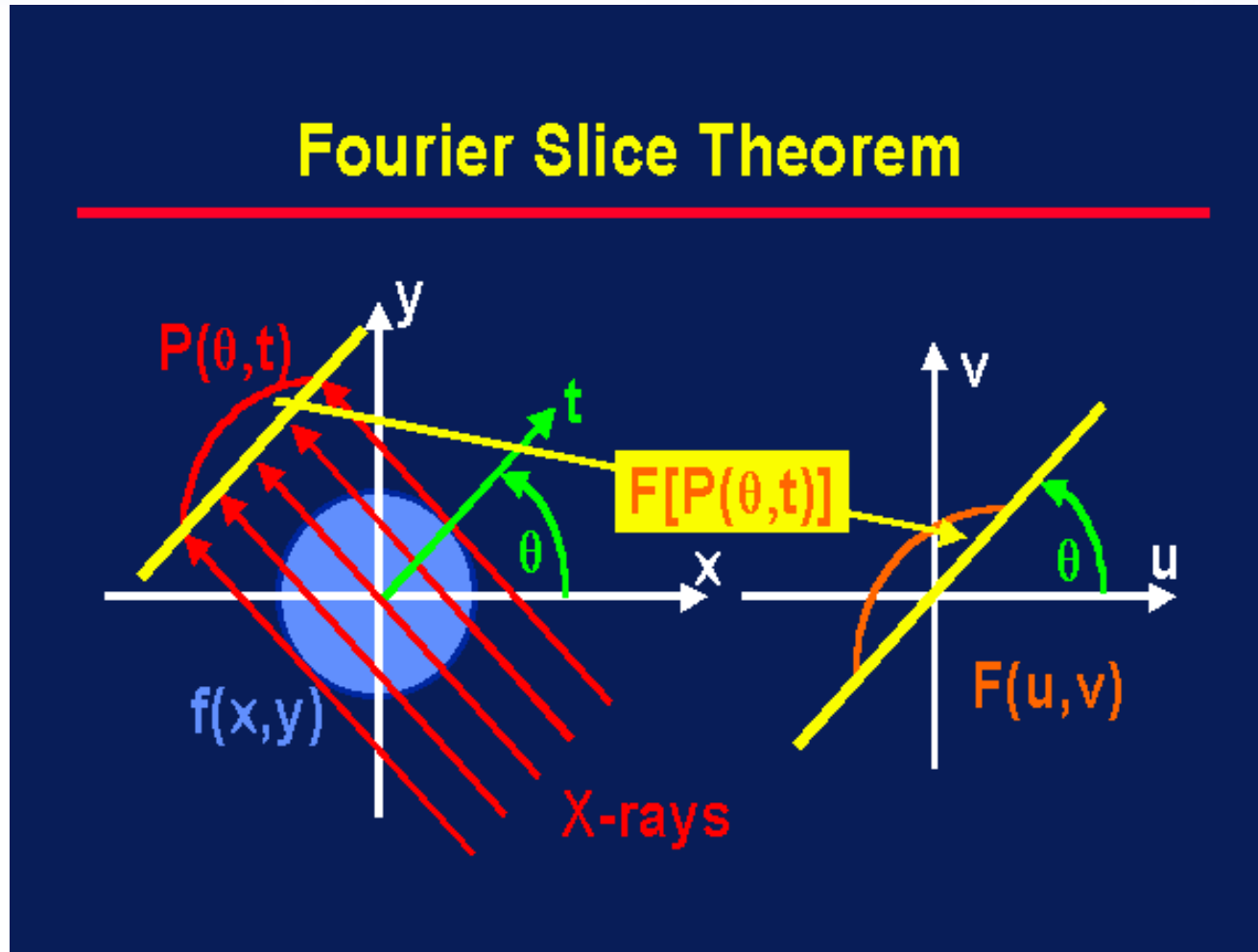
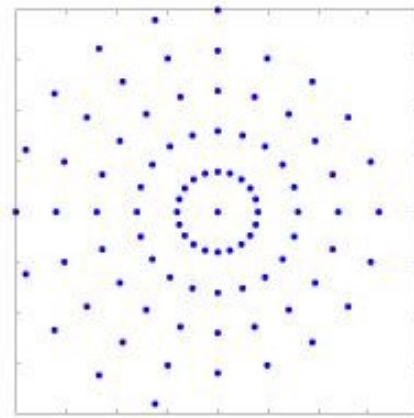


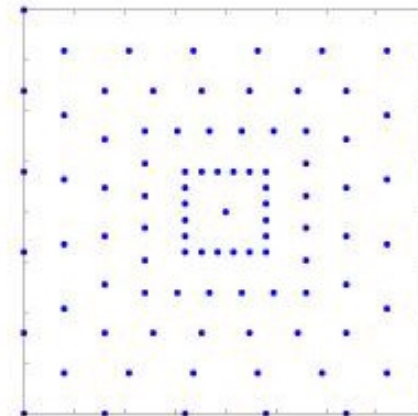
Image reconstruction with NFFT

$$f = F_2^{-1} F_1 g$$

Interpolation from the polar grid
to the Cartesian is required



Linogram (“pseudo-polar”) grid



Nonequispaced Fast Fourier transform (NFFT) can be used

Potts *et al*, 2001

FBP and BPF algorithms

$$f = \left(A^* A \right)^{-1} A^* g = A^* \left(A A^* \right)^{-1} g$$

$$F_2 \left[\left(A^* A \right)^{-1} \delta \right] = \sqrt{\xi^2 + \eta^2}$$

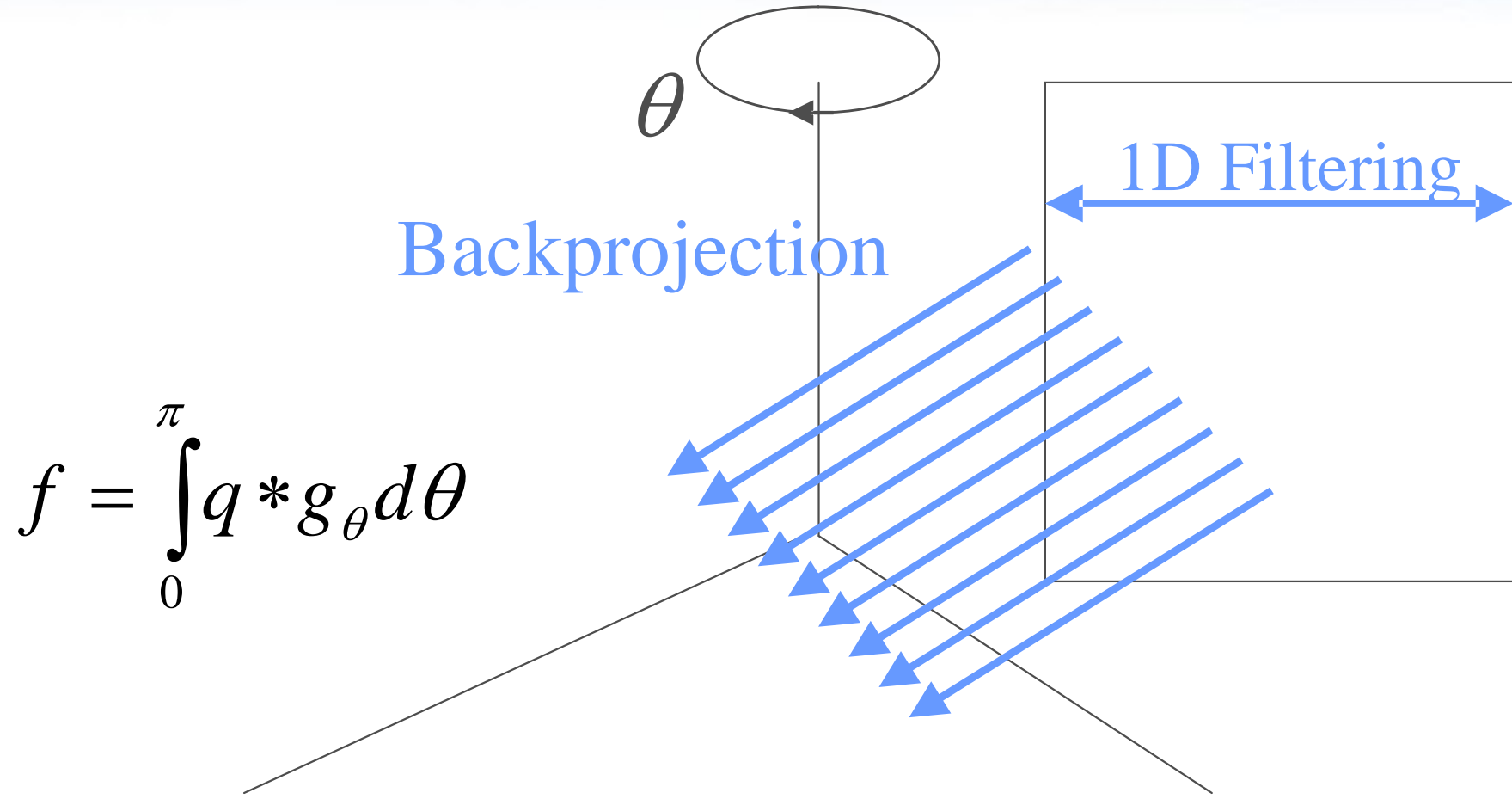
$$F_1 \left[\left(A A^* \right)^{-1} \delta \right] = |\xi|$$

“ramp filter”

$$f = \frac{1}{\pi} F_2^{-1} \left[\sqrt{\xi^2 + \eta^2} \right] \otimes \otimes \int_0^\pi g_\theta d\theta$$

$$f = \frac{1}{\pi} \int_0^\pi F_1^{-1} [|\xi|] \otimes g_\theta d\theta$$

FBP algorithm



Local (“Lambda”) tomography

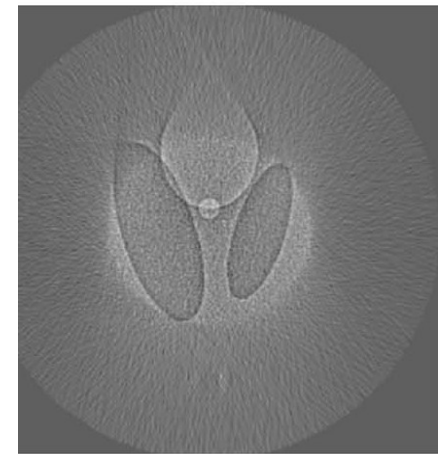
$$F_1^{-1}[\xi|\hat{g}] = H \frac{\partial}{\partial s} g \quad f = A^* H \frac{\partial}{\partial s} g$$

$\frac{\partial}{\partial s} g$ Local operator

$$f_\Lambda = A^* \frac{\partial}{\partial s} g$$

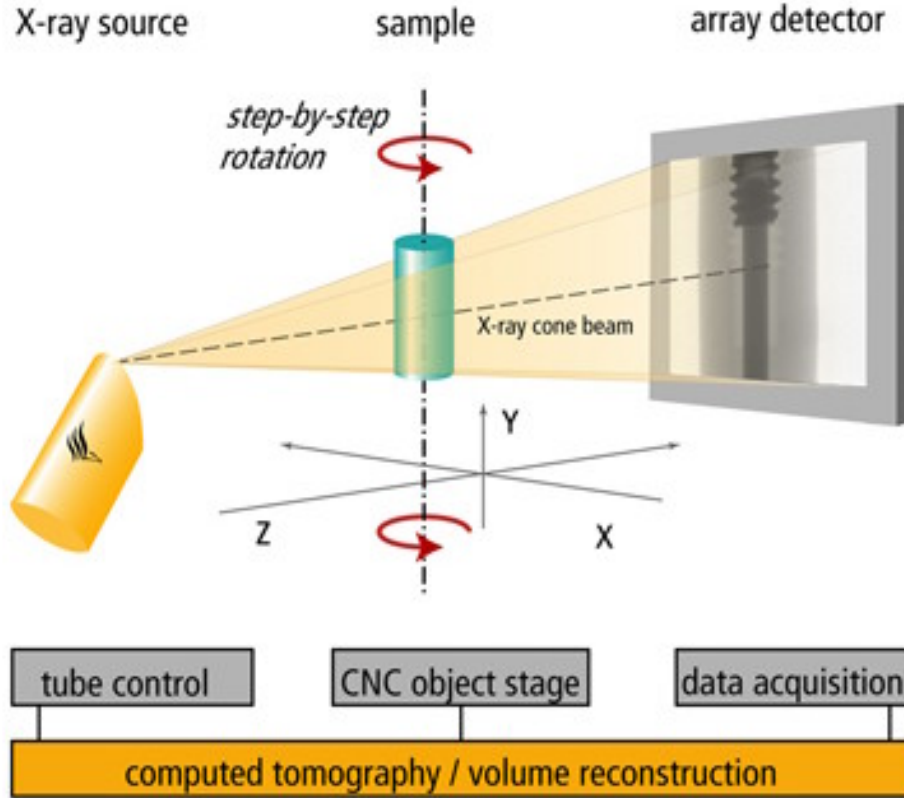
Hilbert transform is non-local:

$$Hg(s) = \frac{1}{\pi} \int_{-\infty}^{\infty} \frac{g(t)}{s-t} dt$$



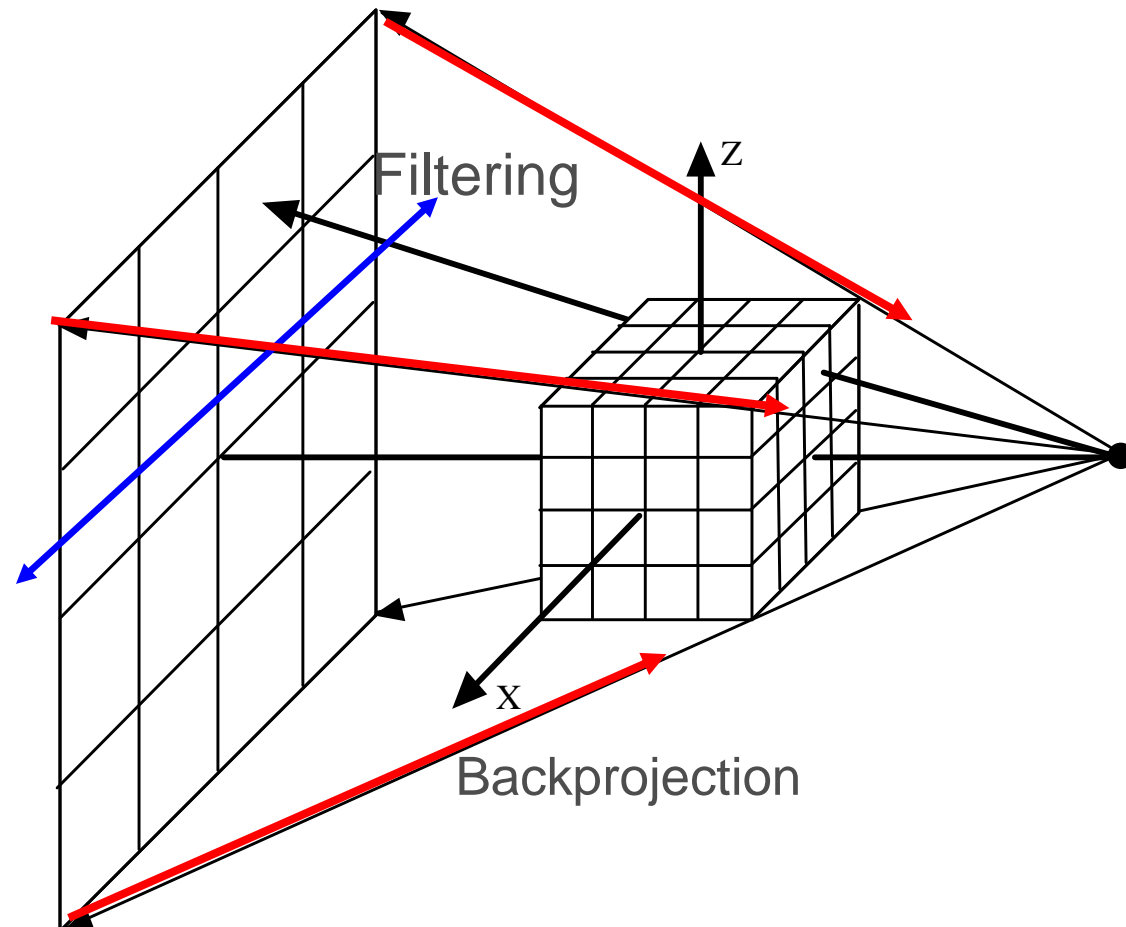
Cone-beam geometry (Microfocus x-ray tube)

Feldkamp algorithm with a circular orbit

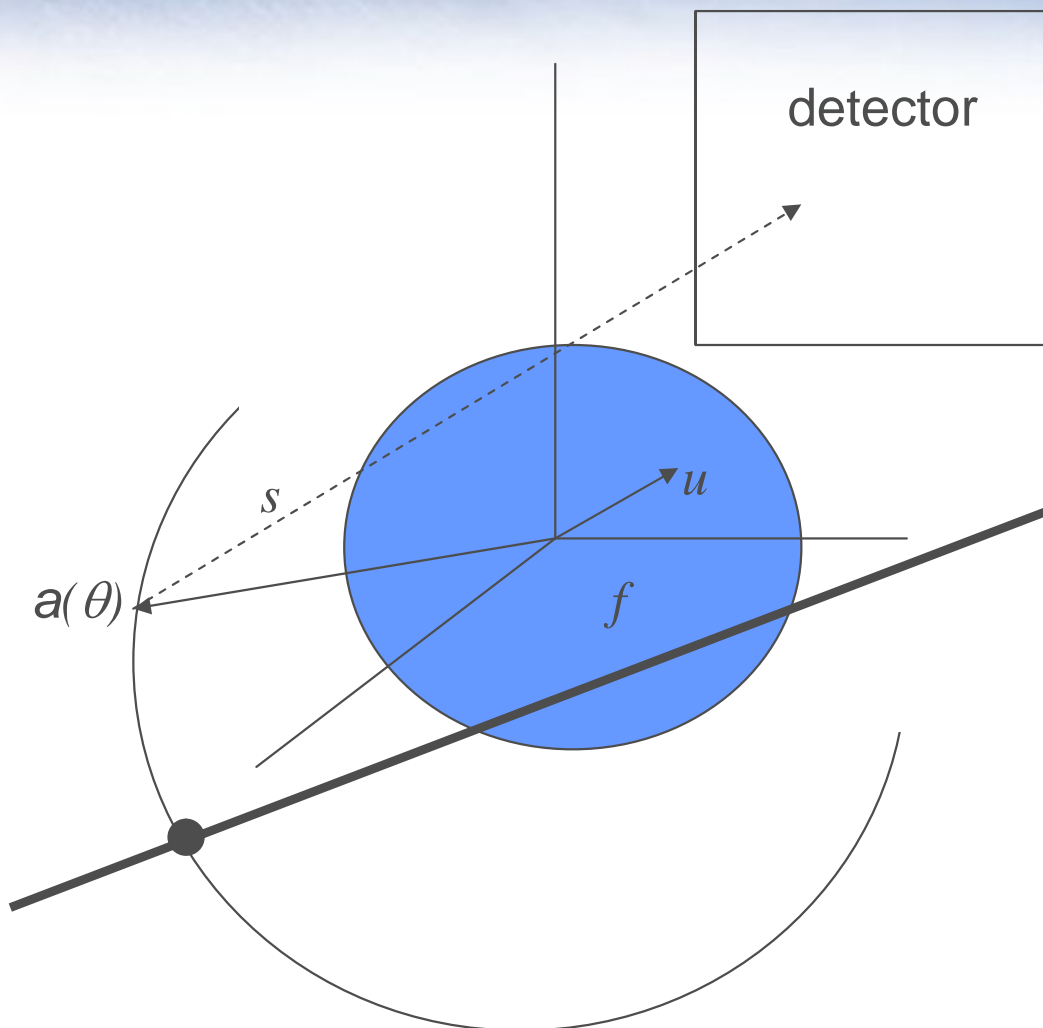


$$f = \int_0^{\pi} q * g_{\theta} d\theta$$

Feldkamp, Davis, Kress, 1984



Kirillov-Tuy condition

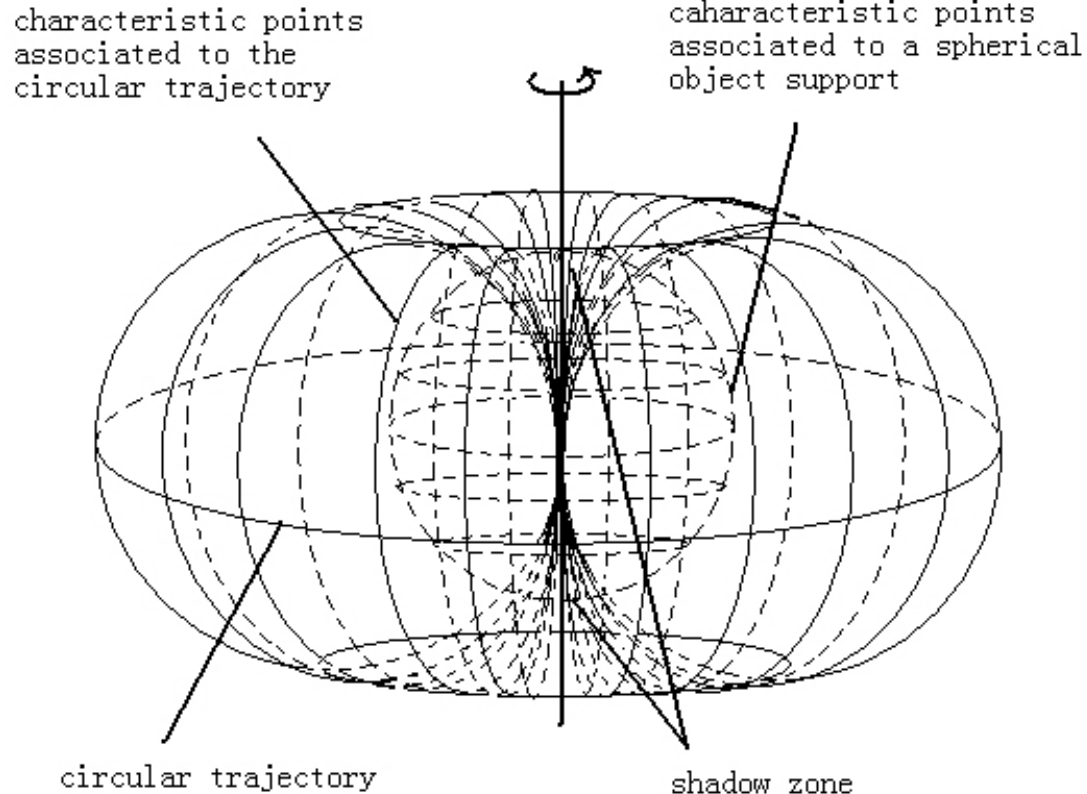


Exact 3D reconstruction
is possible if every plane through
the object intersects the source
trajectory at least once

$$g(a(\theta), u) = \int_0^\infty f(a(\theta) + su) ds$$

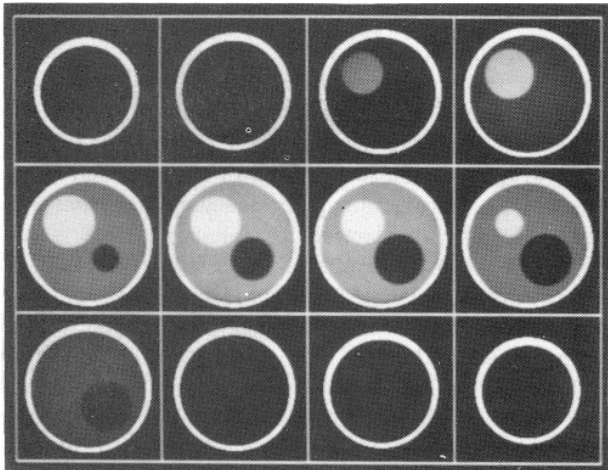
x-ray source trajectory; parametrized as $a(\theta)$

Circular source orbit: artifacts



Bronnikov 1995, 2000

Slices of 3D reconstruction of a phantom (cone angle 30 deg):

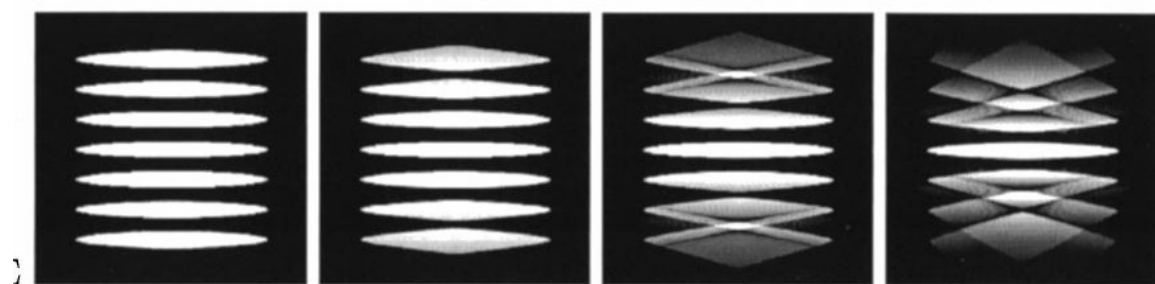


$R = 12.0$

$R = 6.0$

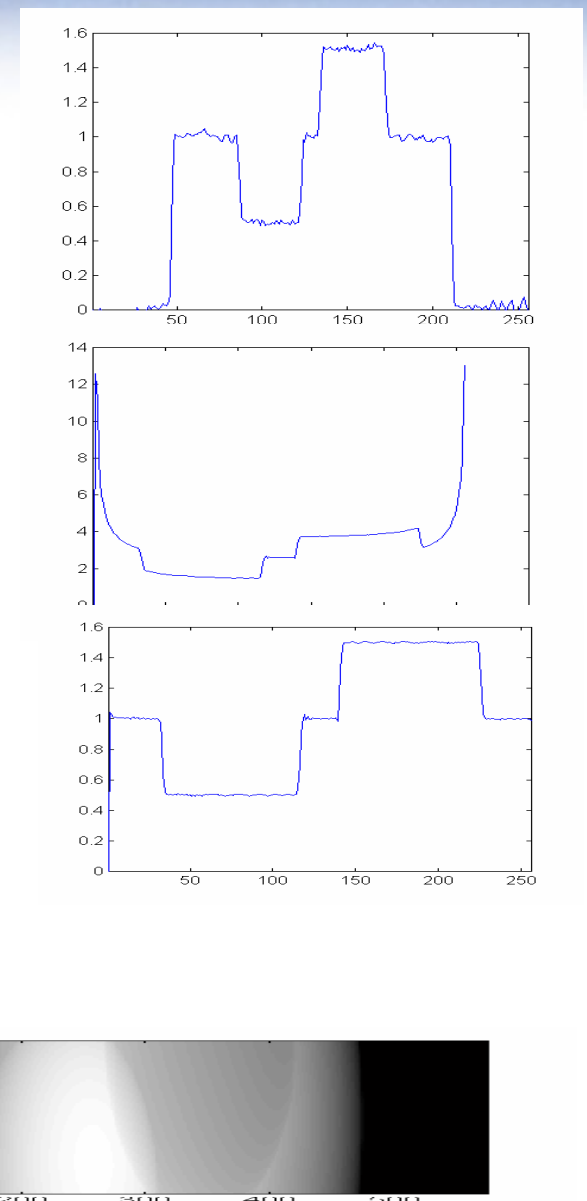
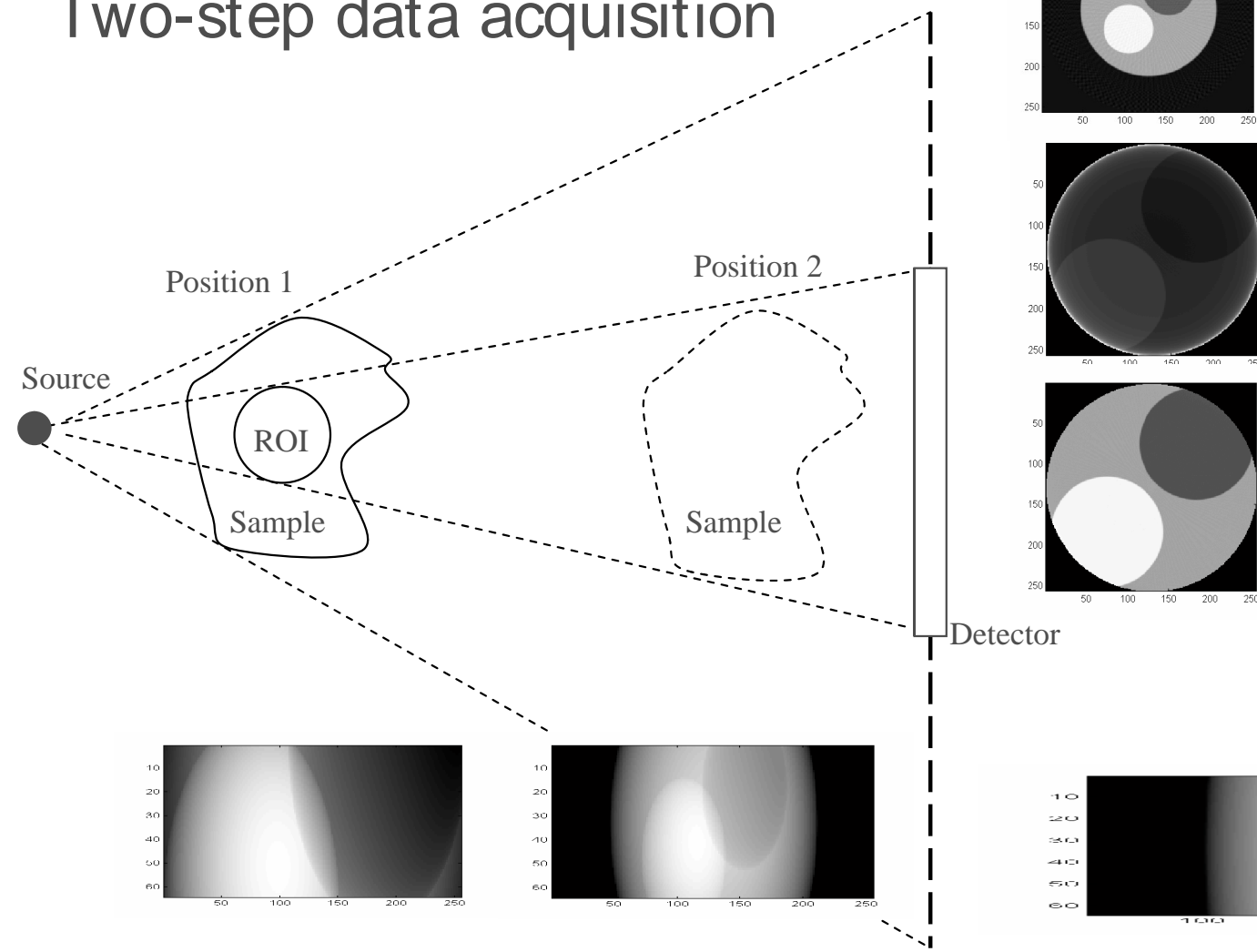
$R = 3.0$

$R = 1.5$

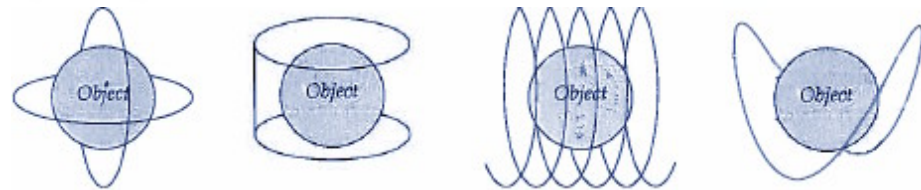


ROI reconstruction

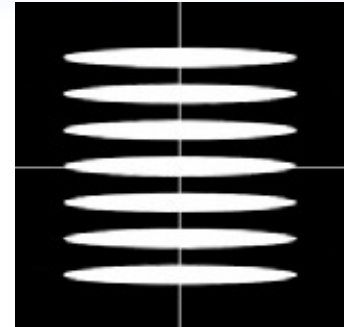
Two-step data acquisition



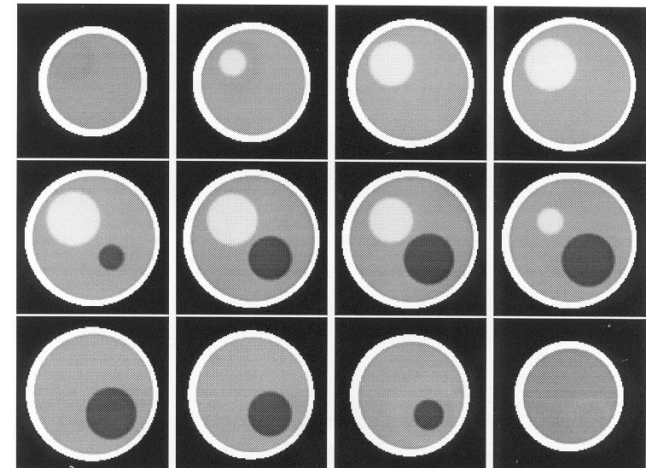
Non-planar source orbits



Non-planar
3D reconstructions
of a phantom:



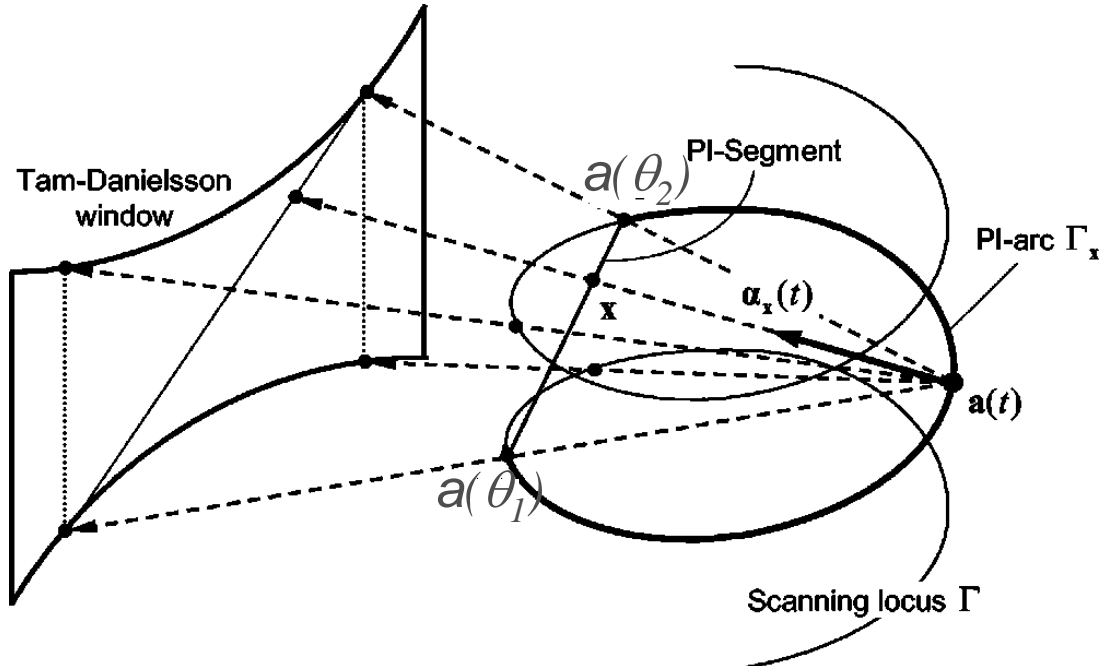
- two orthogonal circles
- two circles and line
- helix (most feasible mechanically)
- saddle



Non-planar orbits satisfy the Kirillov-Tuy condition,
but special reconstruction algorithms are required

Katsevich algorithm for a non-planar source orbit

Katsevich, 2002



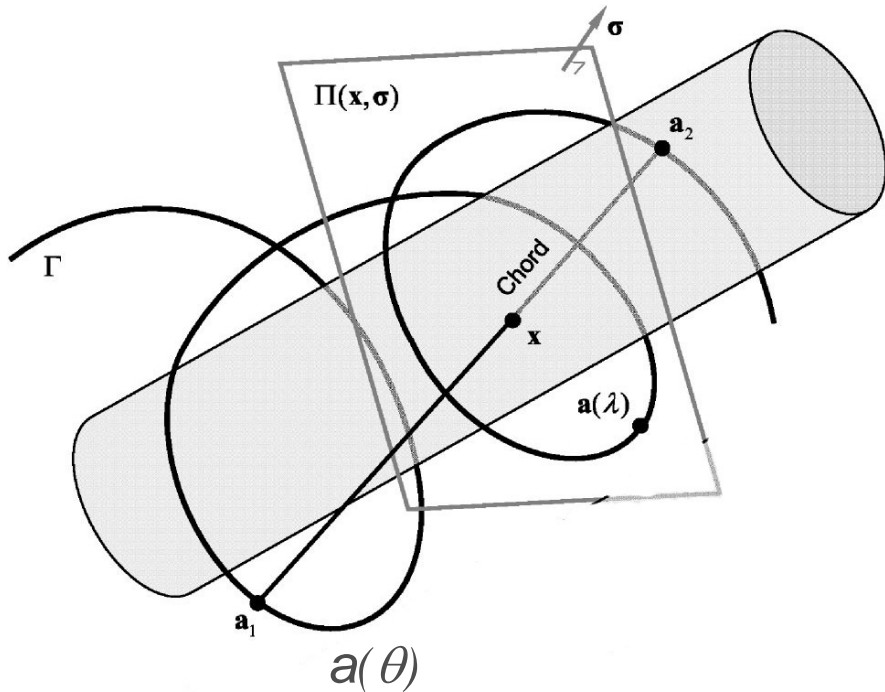
$$f = \frac{1}{2\pi} A^* H_\pi \frac{\partial}{\partial \theta} g$$

1. Differentiation of data
2. Hilbert transform along the filtration lines inside the Tam-Danielsson window
3. Backprojection

PI-line (“segment”, “chord”) between $a(\theta_1)$ and $a(\theta_2)$: $\theta_2 - \theta_1 = 2\pi$

Helix:
$$\mathbf{a}(\theta) = \left(R \cos \theta, R \sin \theta, \frac{h\theta}{2\pi} \right)^T$$

BPF algorithms for ROI reconstruction



$$f = \frac{1}{2\pi} H_\pi A_\pi^* \frac{\partial}{\partial \theta} g$$

1. Differentiation of data
2. Backprojection onto the PI chord (locality!)
3. Hilbert transform along the PI chord

Using that f has the finite support and

$$H H g = -g$$

Zou, Pan, Sidky, 2005 derived:

$$f = \frac{1}{2\pi} H_{\pi, a_1 - a_2}^{-1} A_\pi^* \frac{\partial}{\partial \theta} g$$



Ultra-fast implementation

- Graphic card (GPU)
- CPU

Reconstruction of a 512x512x512 image from 360 projections:

CPU (~2 GHz) :	Single	Dual core	Quad core	Twin quad-core
Time :	~80 sec	~40 sec	~20 sec	~10 sec

Reconstruction of a 1024x1024x1024 image from 800 projections:

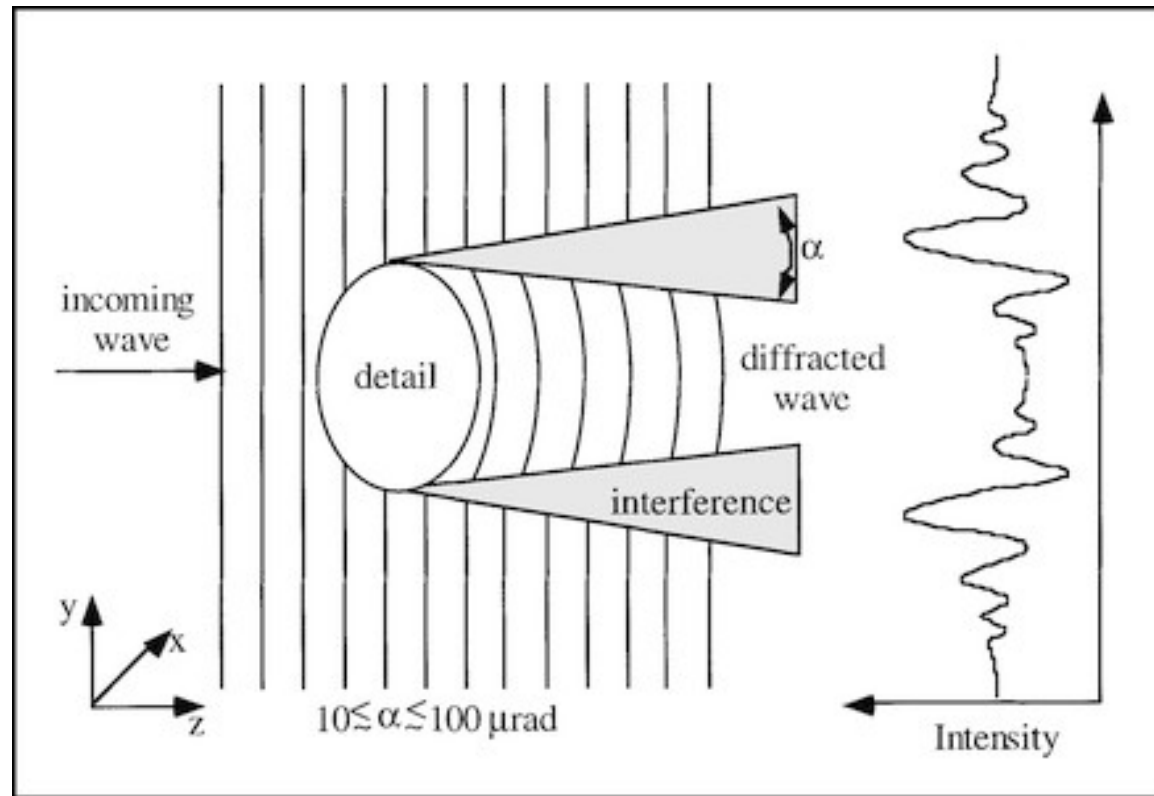
CPU (~2 GHz) :	Dual core	Twin quad-core
Time :	~480 sec	~120sec

Phase-contrast microtomography (Free propagation mode)

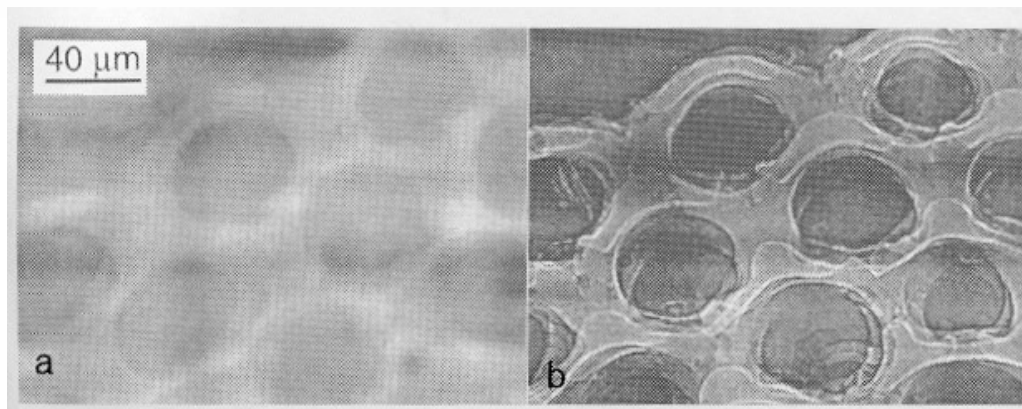
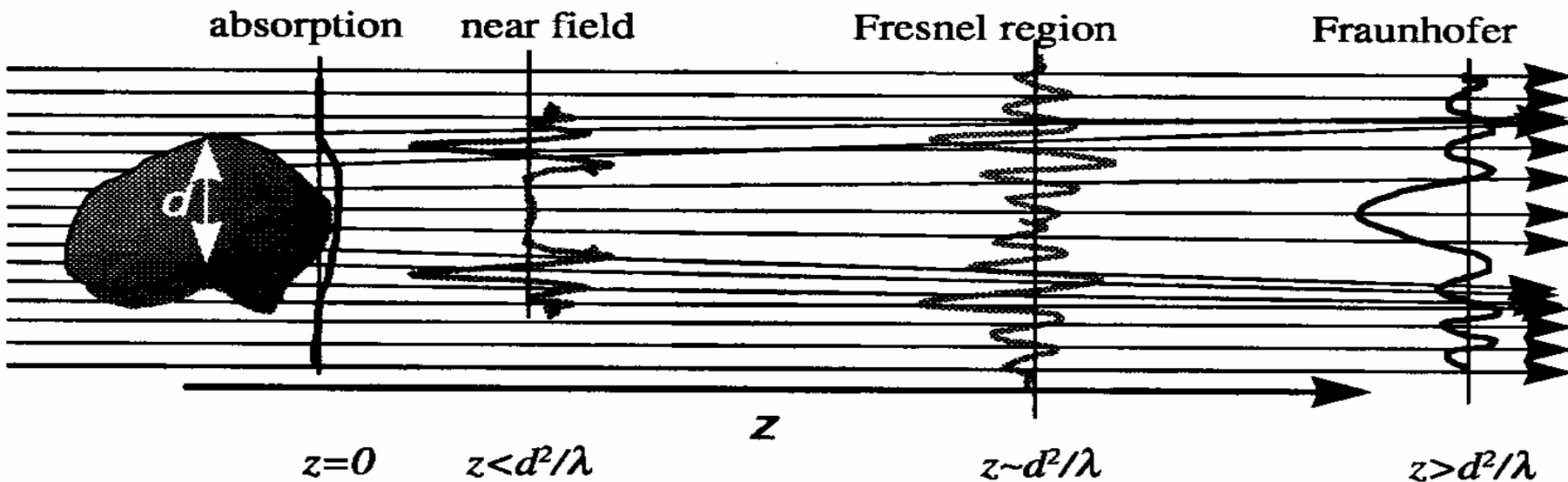
Phase contrast

72

Interference of the phase-shifted wave with the unrefracted waves

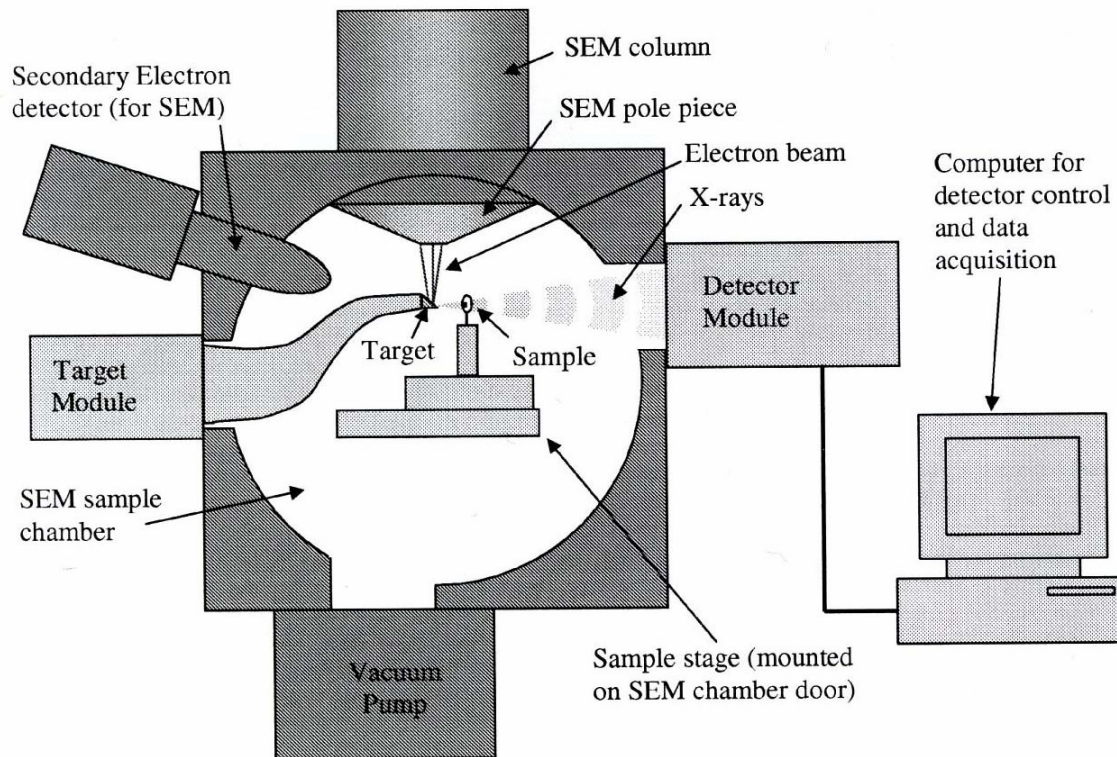


Inline phase-contrast imaging



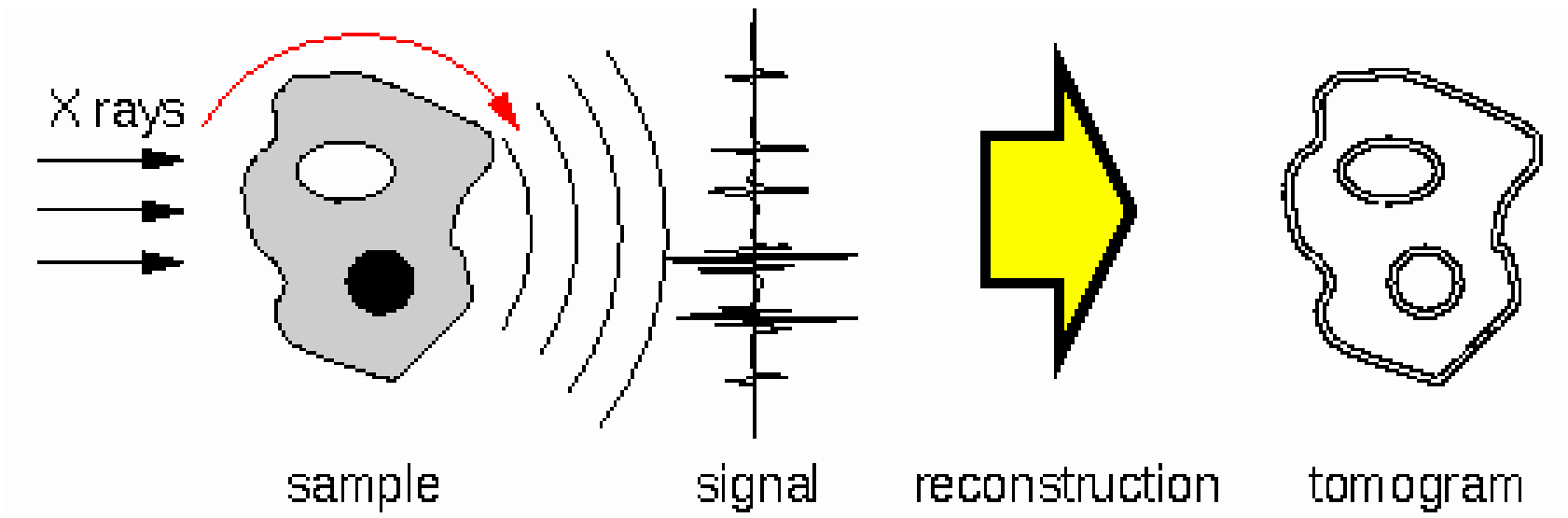
Snigirev et al, 1995

Polychromatic x-ray phase contrast



Wilkins *et al*, 1996

Phase-contrast tomography with Radon inversion: edges



Inverse problem of phase-contrast microtomography

Object function: $f = n - 1$

find $f(x_1, x_2, x_3)$ from $I_\theta^z(x, y), \quad 0 \leq \theta < \pi$

- CTF (Cloetens *et al*, 1999)
 - TIE (Paganin and Nugent, 1998)
 - Weak-absorption TIE (Bronnikov, 1999) FBP, single detection plane
- } Phase retrieval,
more than one detection plane

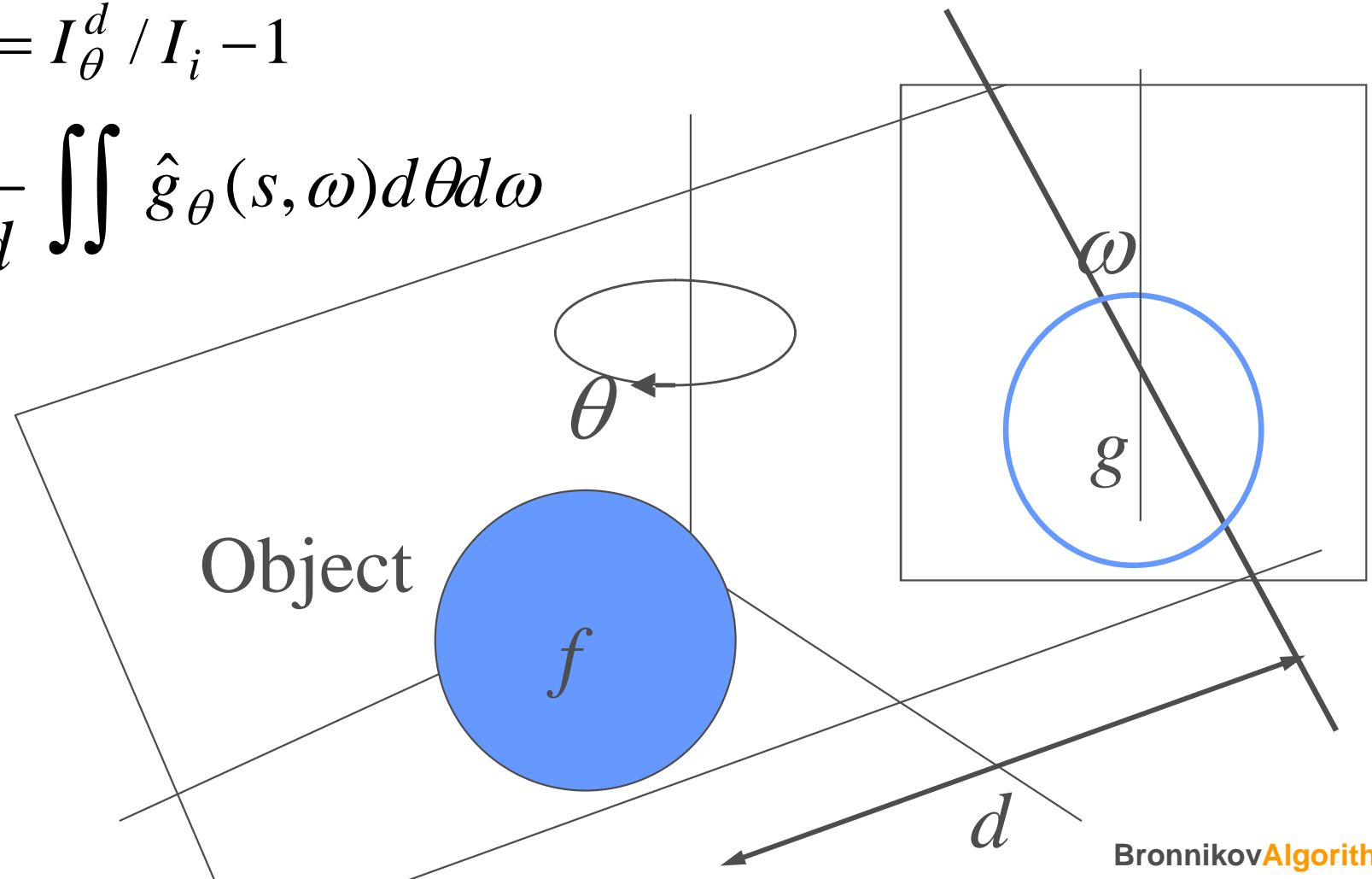
Radon transform solution of TIE

$$I_\theta^d(x, y) = I_\theta^0 \left[1 - \frac{\lambda d}{2\pi} \nabla^2 \varphi_\theta(x, y) \right]$$

Bronnikov, 1999

$$g_\theta(x, y) = I_\theta^d / I_i - 1$$

$$f = \frac{1}{4\pi^2 d} \iint \hat{g}_\theta(s, \omega) d\theta d\omega$$



Phase-contrast reconstruction in the form of the FBP algorithm

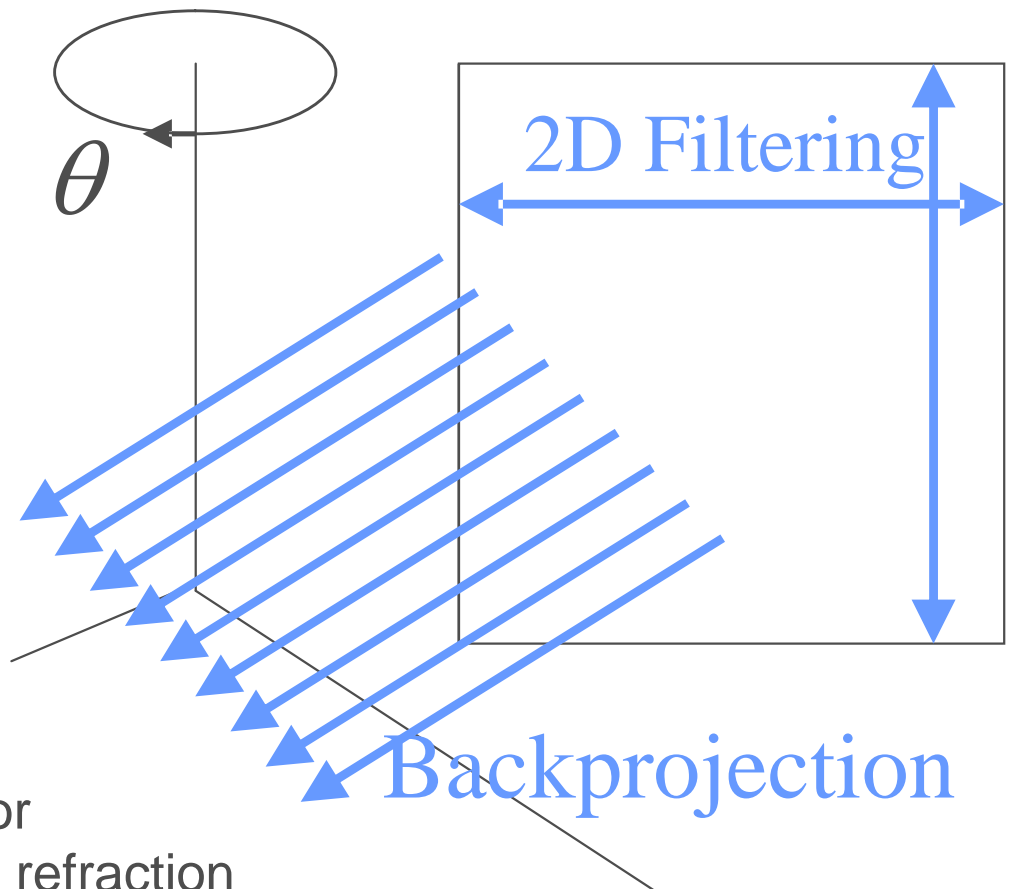
Bronnikov, 1999, 2002, 2006

$$f = \frac{1}{4\pi^2 d} \int_0^\pi q * * g_\theta d\theta$$

$$q = \frac{|y|}{x^2 + y^2}$$

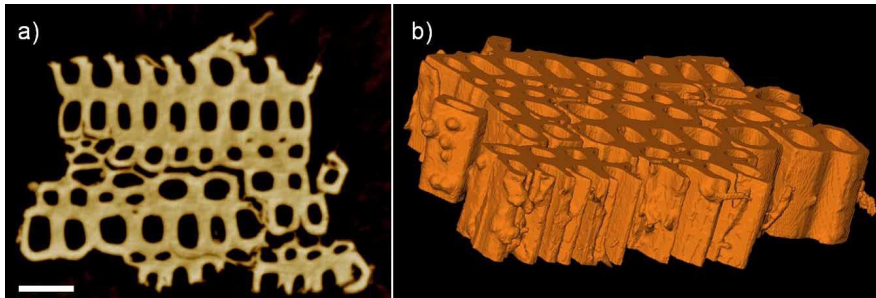
$$Q = \frac{|\xi|}{\xi^2 + \eta^2}$$

$$Q_\alpha = \frac{|\xi|}{\xi^2 + \eta^2 + \alpha}$$



Gureyev *et al*, 2004: choice of α for
linearly dependent absorption and refraction

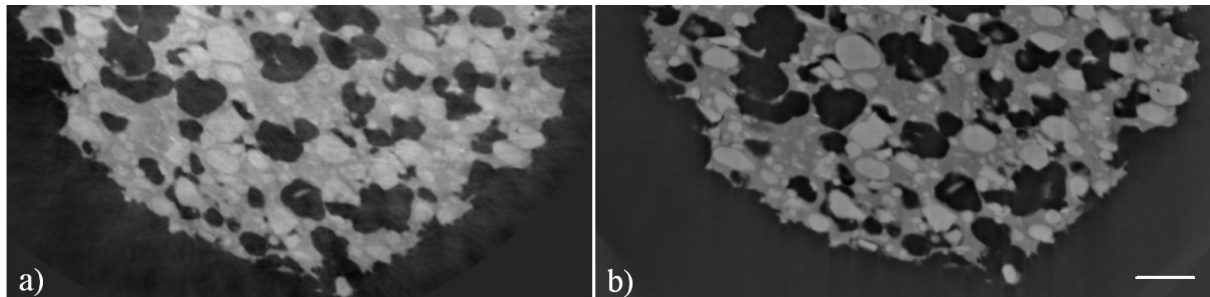
Implementation at SLS



Phase tomography reconstruction (a) and the 3D rendering (b) of a 350 microns thin wood sample using modified filter given in the Eq. (8). The length of the scale bar is 50 μm .

“MBA: Modified Bronnikov Algorithm”
Groso, Abela, Stampanoni, 2006

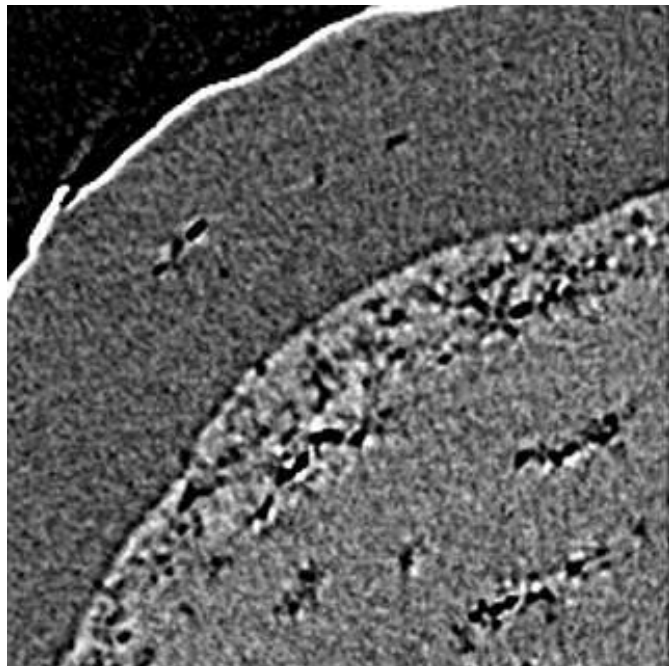
$$Q_\alpha = \frac{|\xi|}{\xi^2 + \eta^2 + \alpha}$$



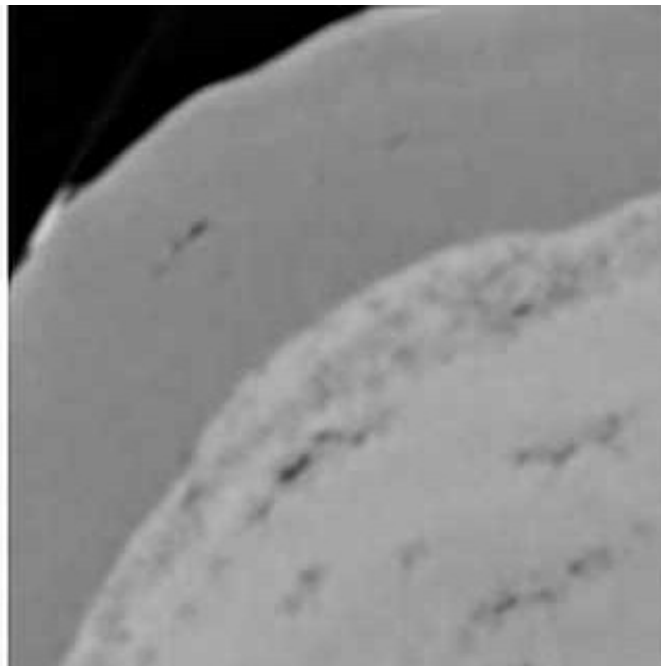
Validation of the MBA method: (a) Phase tomographic reconstruction of sample consisting of polyacrylate, starch and cross-linked rubber matrix obtained using DPC and (b) using MBA. The length of the scale bar is 100 μm .

Implementation at Ghent University

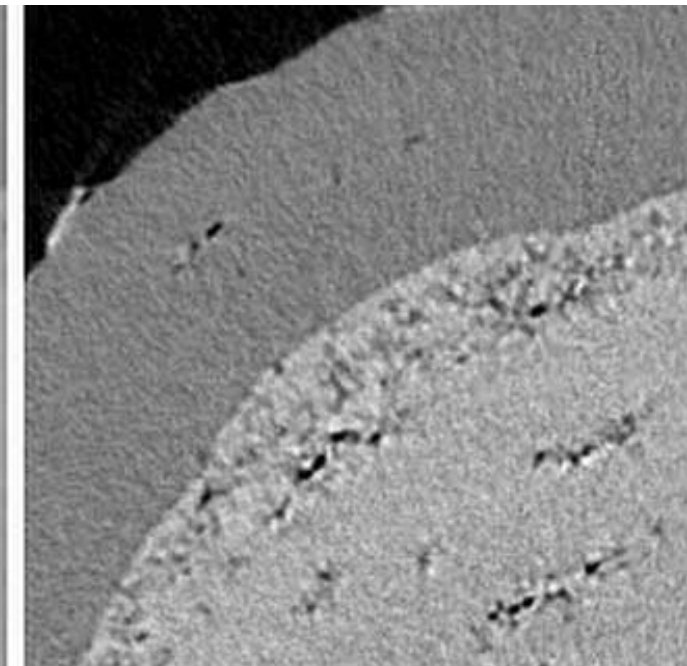
De Witte, Boone, Vlassenbroeck,
Dierick, and Van Hoorebeke, 2009



Radon inversion



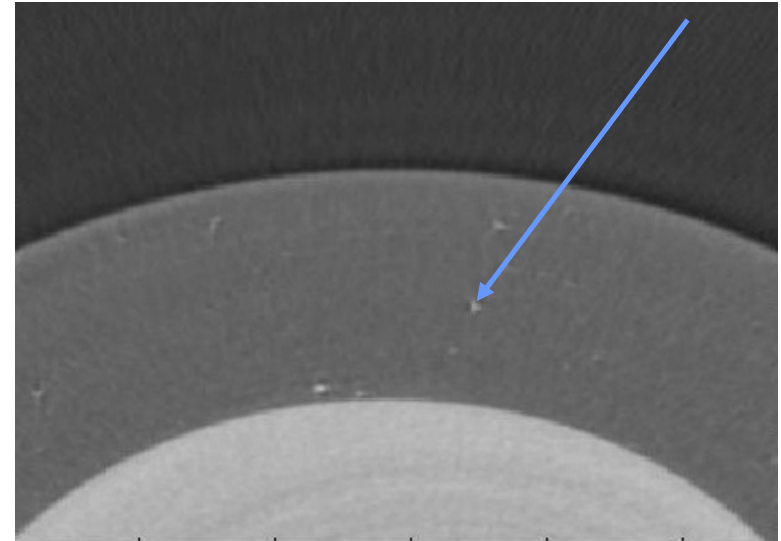
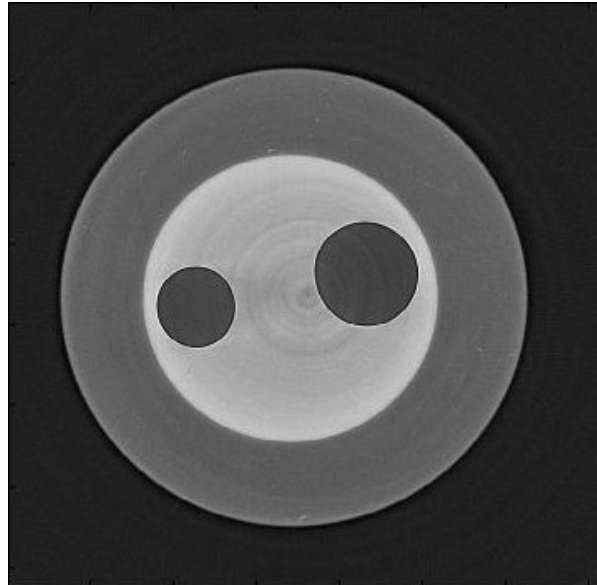
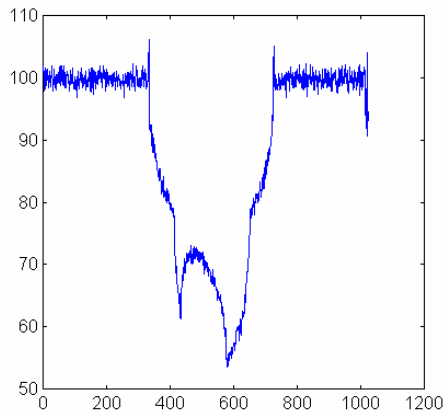
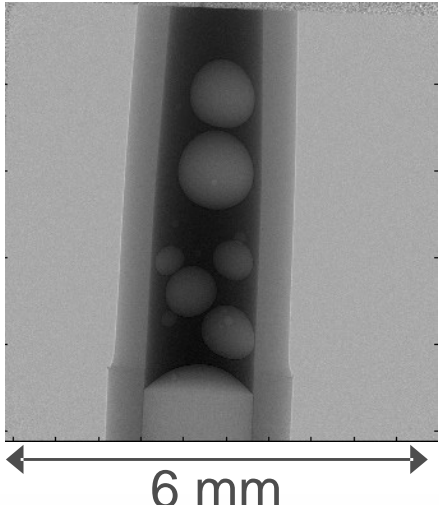
“Modified Bronnikov Algorithm”



“Bronnikov-Aided Correction”

Polychromatic source, mixed phase and amplitude object

Air bubbles in epoxy,
relatively strong absorption:



Reconstruction by the “Bronnikov Filter” with correction

Data provided by Xradia

Summary

- New developments in theory:
 - parallel-beam CT (synchrotron): the use of NFFT
 - cone-beam CT (microfocus): exact reconstruction with non-planar orbits; exact ROI reconstruction
(Katsevich formula, PI line, Hilbert transform on chords)
- New developments in implementation:
 - ultra-fast 3D reconstruction on multicore processors
 - (1024^3 voxels within one-two minutes on a PC)
- New developments in coherent methods:
 - robust algorithms for 3D phase reconstruction
 - correction for the phase component